Electron detachment in low-energy collisions of H^- and D^- with He†

S. K. Lam, J. B. Delos, R. L. Champion, and L. D. Doverspike
Department of Physics, College of William and Mary, Williamsburg, Virginia 23185
(Received 26 December 1973)

Measurements and calculations have been made of elastic scattering and electron detachment in collisions of H^- and D^- with He at energies of 5–120 eV. The measurements show no other inelastic processes occurring in this energy range. The mechanism responsible for electron detachment is assumed to be the crossing of the H^- bound state with the continuum of free states; the bound state is then assigned a complex energy. The measured elastic scattering differential cross section shows no structure except at $E\theta \sim 200$ eV deg, where there is a region of downward curvature in the graph of $\log\sigma$ vs θ. This is interpreted as the threshold angle for electron detachment, and it is directly related to the crossing point. By empirically fitting the experimental differential cross section, the general features of the complex potential were obtained. By using the resulting potentials, the total detachment cross section was calculated and compared to the experimental results of Bailey, May, and Muschlitz. Only fair agreement is found at low energies, and poor agreement at higher energies (>100 eV). The theory predicts an isotope effect in the elastic differential cross section, and this effect provides a test of the theory. A careful series of experiments at 20 eV displayed the effect. A preliminary measurement of the electron energy spectrum was also made.

I. INTRODUCTION

A. Objective

The mechanism for collisional detachment of electrons from negative ions,

$$A^- + B \rightarrow A + B + e^-, \tag{1}$$

is very well known but it is not yet well enough understood. As the negative ion approaches the target atom, the energy of the bound state of the electron rises until it crosses or becomes degenerate with the continuum of states representing neutral atoms and a free electron. At this point, it is said that the energy acquires a width $\Gamma(R)$, and the state decays in time as detachment occurs. In principle, it is possible to calculate the potential and the width *ab initio*,[1] and when this is done, it is a simple matter to derive theoretical expressions for the survival probability of the negative ion, the differential cross section for elastically scattered ions and neutral products, and the energy spectrum of detached electrons.

While the theory is plausible, it does not yet rest upon a firm experimental or theoretical foundation; it has not yet been subjected to a critical theoretical or experimental test. *Ab initio* calculations have been carried out only on the H_2^- system[2–4]; electron scattering from H_2 has confirmed the theoretically predicted isotope effect, but such experiments give limited information about the detachment process. A much better test could be obtained from low-energy differential scattering measurements.

One of the simplest systems is He-H^-, and an *ab initio* calculation on this system is now being carried out.[5] The purpose of this paper is to test the applicability of the complex-potential theory to H^--He collisions. We have measured the elastic differential cross section for H^--He collisions for energies from 5 to 120 eV, and have also made a preliminary measurement of the energy spectrum of detached electrons. Interpreting our results in terms of the complex-potential theory, we are able to determine the crossing point, the general shape of the HeH^- potential curve and the behavior of $\Gamma(R)$. We have also found an isotope effect that is compatible with the complex-potential theory. Finally, we have calculated the total detachment cross section and compared it to experiment.

B. Relationship to other work

In an elegant series of experiments, Risley and Geballe[6] have measured the elastic differential cross section and the differential and total cross sections for electron detachment for H^- on He (and other systems) at energies from 0.2 to 10 keV. Although a complete theoretical analysis of their data has not yet been made, their tentative conclusion is that the complex-potential method does not apply in their high-energy range. This would not be surprising; in their experiments the incident ion velocity is not much less than the

electron velocity, so the adiabatic picture might not be valid. But at the low energies involved in our experiments, we expect the Born-Oppenheimer picture to provide a reasonable starting point, and it is possible that the complex-potential formalism may apply.

Processes analogous to collisional detachment, involving strong interaction between a discrete bound state and a continuum of free states, are currently of great interest, because they appear in many branches of physics and chemistry. In the upper atmosphere, the rate of loss of electrons in the E layer is dominated by dissociative recombination[7] of electrons with positive molecular ions:

$$e^- + AB^+ \rightarrow A + B\,. \tag{2}$$

In the D layer, the creation and loss of negative ions are in some cases dominated by dissociative attachment or associative detachment[8]:

$$e^- + AB \rightleftarrows A^- + B\,. \tag{3}$$

Both of these processes are obviously directly related to collisional detachment (1). Similarly, in high-temperature flames, negative ions are known to be very abundant, but their role is not understood.[9] Presumably they are formed and destroyed by these same mechanisms.

In cosmological studies, some of the controversial speculations about the existence of antimatter on a large scale may be resolved by an examination of matter-antimatter collisions leading to rearrangement and annihilation:

$$\mathrm{H} + \overline{\mathrm{H}} \rightarrow p\bar{p} + e\bar{e} \rightarrow \text{products}. \tag{4}$$

These processes also occur through the same mechanism,[10] involving a bound state crossing or joining a continuum. While potential curves for some of these processes have been calculated by Bardsley and others,[10] one of the significant remaining problems is the calculation of the reaction probability by quantum or semiclassical methods.

In another branch of astronomical investigation, it has been proposed that the formation of molecules in interstellar space takes place through negative ions as intermediates.[11] If this is true, then these molecules are formed through a sequence of reactions like (1) and (3), and a calculation of the rates of these reactions is contingent upon a satisfactory understanding of the mechanism.

Finally, in relativistic quantum mechanics and quantum electrodynamics, there is considerable interest in the x-ray spectra of superheavy atoms, and especially in the possibility of positron production in a close collision between two heavy atoms.[12] As the two nuclei approach closely, they effectively become a "united atom" of very high charge. The energy of an inner-shell electron then decreases until it may cross the negative-energy Dirac "sea" of electrons. A hole in this bound state may become filled by an electron from the "sea", leaving a free hole, i.e., an escaping positron.

All of the above processes are believed to occur through the same mechanism: the crossing of a discrete state with a continuum. So it is unfortunate that the theoretical description of this mechanism remains incomplete. We present here a test of the validity and applicability of this theory to negative-ion collisions.

II. THEORY

A. Complex-potential description

The potential-energy curve for H or D interacting with He has been the subject of several theoretical and experimental studies,[13] and is now known quite accurately. For $1a_0 < R < 5a_0$, it is well described by the function

$$V_2(R) = 39.04e^{-1.53R},$$

where V and R have units of eV and bohr, respectively. Since the electron can have any non-negative kinetic energy ϵ, we can regard the total electronic energy of the (He + H + free e^-) system as a continuum of parallel curves. Qualitative features of the potential curves are indicated in Fig. 1; E is the total energy of the system, ϵ is the energy of the free electron, and K is the asymptotic kinetic energy of the nuclei.

At infinite separation, the HeH^- electronic energy lies 0.75 eV below the HeH curve. A definitive calculation of the curve is not yet available, but an early calculation by Browne and Dalgarno[14] indicates that it approaches the HeH curve at a distance R_x of about $3a_0$. For small separations, the HeH^- curve is believed to lie in the continuum of HeH + free e^- curves, and so it can no longer be regarded as a bound state, but rather as a quasibound resonance. Since the electron has enough energy, it will eventually escape, so the boundary condition on the electronic wave function is that it be purely outgoing at large distances. It can therefore be described as a decaying state with a complex energy,

$$E(R) = V_1(R) - \tfrac{1}{2}i\Gamma(R), \tag{5}$$

with $\Gamma(R)$ inversely proportional to the lifetime of the state. (The formalism does not include the possibility of excitation of higher resonances; our experiments have shown no evidence of such excitations, though they do appear in the higher-

energy experiments of Risley and Geballe.)

Because of the short wavelength associated with the nuclear motion, the cross section can be calculated by a semiclassical approach; furthermore, since the potentials are purely repulsive, there are no interference effects, so that completely classical arguments are sufficient. From the standard relation between scattering angle and impact parameter,

$$\Theta(b) = \pi - 2b \int_{R_0}^{\infty} \frac{dR}{R^2[1 - V_1(R)/E - b^2/R^2]^{1/2}} , \quad (6)$$

the cross section in the absence of detachment is determined from $V_1(R)$ in Eq. (5) as

$$\sigma_0(\theta) = -\frac{b\,db}{\sin\theta\,d\theta} . \quad (7)$$

B. Elastic differential scattering cross section

Within this semiclassical approach,[15a] the probability that the electron does *not* detach (survival probability) is given by

$$P_s(\theta) = \exp\left(-\int_{-\infty}^{\infty} \Gamma\,dt\right)$$

$$= \exp\left(-2\int_{R_0}^{\infty} \frac{\Gamma(R)dR}{v_R}\right) . \quad (8)$$

This quantity depends on impact parameter b and hence scattering angle θ through the dependence on the classical turning point R_0, and the radial velocity v_R, which is given by

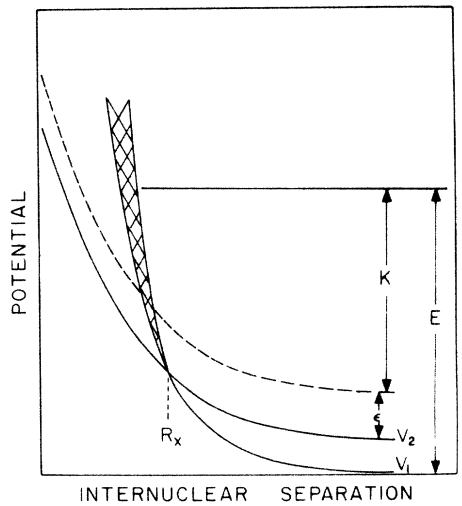

FIG. 1. Schematic illustrations of the potential curves involved in the electron-detachment process. The shaded area represents the width $\Gamma(R)$ of the HeH^- state (V_1), and the dashed line represent one of the continuum states of HeH + a free electron (with kinetic energy = ϵ).

$$v_R = v_\infty\left(1 - \frac{V_1(R)}{E} - \frac{b^2}{R^2}\right)^{1/2} .$$

Accordingly the detachment probability can be written as

$$P_d(\theta) = 1 - P_s(\theta) .$$

The differential cross section for elastic scattering is then given by

$$\sigma_{el}(\theta) = \sigma_0(\theta)P_s(\theta) . \quad (9)$$

We can immediately visualize the qualitative behavior of the elastic cross section. At large impact parameters, the H^- never penetrates into the detachment region; hence electron detachment would be classically forbidden, so at small $E\theta$, the cross section is completely elastic. At smaller impact parameters, detachment is possible, so at large $E\theta$ the elastic cross section is less than σ_0. When $R_0 = R_x$, we are at the threshold for detachment. However, it must be recognized that this threshold is not a sharp point: For R_0 slightly greater than R_x, detachment can still take place through nonadiabatic effects, and for R_0 less than R_x, the survival probability must decrease smoothly. This means that $\Gamma(R)$ must decrease smoothly as R increases to R_x. However, the behavior of $\Gamma(R)$ at R_x is problematic. In a completely rigorous treatment, one would expect to find that $\Gamma(R)$ goes linearly to zero at R_x; detachment occurring for $R_0 > R_x$ would have to be described in a different framework. However, we believe it is possible to account for this classically forbidden detachment in a nonrigorous way by allowing $\Gamma(R)$ to be small but not zero for $R > R_x$. In any case, the detachment threshold would not be manifested as a sharply defined feature in the differential cross section, but rather as a region whose width depends upon the precise behavior of $\Gamma(R)$ near R_x. These features are illustrated in Fig. 2.

As is well known, the theory also predicts the existence of an isotope effect.[15b] For purely elastic scattering, Eq. (6) shows that the differential cross section in the center-of-mass frame does not depend on the mass, but only on the center-of-mass energy. So in the absence of detachment, at a given center-of-mass energy, H^- and D^- should have exactly the same differential cross section, σ_0. However, at the same energy, they are traveling with different velocities, and the probability of detachment increases with the time spent in the region $R < R_x$. From Eq. (8) we have

$$P_s(\theta) = \exp[-\mu^{1/2} I(\theta)] ,$$

where

$$I(\theta)=\left(\frac{2}{E}\right)^{1/2}\int_{R_0}^{\infty}\frac{\Gamma(R)dR}{[1-V_1(R)/E-b^2/R^2]^{1/2}} \tag{10}$$

and μ is the reduced mass. As a consequence,

$$\frac{\sigma_D(\theta)}{\sigma_H(\theta)}=\exp[(\mu_H^{1/2}-\mu_D^{1/2})I(\theta)], \tag{11}$$

where σ_D and σ_H are the differential elastic cross sections for D^- and H^-, respectively. Since $I(\theta)$ increases as θ increases, it follows that $\sigma_D(\theta)$ should decrease more rapidly than $\sigma_H(\theta)$ as θ increases. The effect is not large, but it can be observed in a careful experiment. The detection of the predicted isotope effect constitutes an important success for the complex-potential theory.

Finally, we mention that Chen[3,4] has proposed a correction to Eq. (8) resulting from a modification of the Airy-function connection formula owing to the complex potential at the turning point. Chen and Peacher[3,4] have also developed a complete formalism based on the solution to the time-independent Schrödinger equation for a complex potential; this approach yields the classical formula (8) as a special case, but it also gives refinements that become important at low energy. We have not incorporated any of these refinements because in the present case, they are very small.

C. Energy spectrum of detached electrons

In the complex-potential description, for a given trajectory the probability that the electron will detach between time t and $t+dt$ is

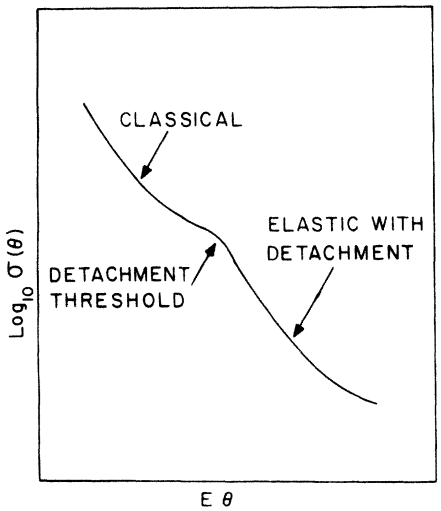

FIG. 2. Qualitative behavior of differential elastic scattering cross section when accompanied by electron detachment.

$$\frac{dP_d}{dt}dt=\Gamma(t)\exp\left(-\int_{-\infty}^{t}\Gamma(\tau)d\tau\right)dt\ . \tag{12}$$

In the classical framework, at each time there is a well-defined position $R(t)$ which determines the energy of the escaping electron through

$$\epsilon(R(t))=V_1(R(t))-V_2(R(t)) \tag{13}$$

(see Fig. 1). Therefore, for each trajectory, the probability that the electron will detach with energy between ϵ and $\epsilon+d\epsilon$ is

$$P(\epsilon,b)d\epsilon=\frac{\Gamma(R(\epsilon))}{(\Delta F)v_R(R(\epsilon))}\left[\exp\left(-\int_{-\infty}^{t_{in}}\Gamma dt\right)+\exp\left(-\int_{-\infty}^{t_{out}}\Gamma dt\right)\right]d\epsilon, \tag{14}$$

where

$$\Delta F=-\frac{d}{dR}(V_1-V_2)\Big|_{R=R(\epsilon)}$$

and v_R is the radial velocity; t_{in} and t_{out} are the two times at which the trajectory passes through the point $R(\epsilon)$, which is obtained by inverting Eq. (13). Finally, integrating over all trajectories, we obtain

$$\sigma_d(\epsilon)=2\pi\int_0^{\infty}P(\epsilon,b)b\,db\ . \tag{15}$$

Two remarks about the behavior of $\sigma_d(\epsilon)$ are especially noteworthy. First, a narrow resonance (small Γ) implies a broad energy spectrum, whereas a large Γ (broad resonance) implies that most of the electrons will come off with a very low energy. In the present case, Γ is large, and most escaping electrons have kinetic energies $\lesssim 0.1$ eV.

Second, we have already mentioned the problem of the behavior of Γ near R_x, and we have argued that $\Gamma(R)$ could be assumed to remain finite (but small) for $R>R_x$. Although such a treatment cannot be completely rigorous, it is interesting to consider its consequences. It is easy to show that if Γ goes to zero at R_x, then the detachment cross section must go to zero as the electron energy goes to zero; if Γ remains finite at R_x, $\sigma_d(\epsilon)$ will remain finite as $\epsilon\to 0$:

$$\sigma_d(\epsilon\to 0)\to\Gamma(R\to R_x)\ .$$

Therefore, the measurement of the limiting behavior of the electron energy spectrum will be especially interesting. (Our experiments, presented in Sec. IV, do not give a definite conclusion.)

Some simple approximations to the electron-energy-spectrum calculation are discussed in the Appendix.

III. EXPERIMENTAL METHOD

The experiment consists of directing a momentum-analyzed beam of H^- (or D^-), which has been produced in a duoplasmatron ion source, into a collision chamber containing target gas at low pressure ($\sim 5\times 10^{-4}$ Torr). The scattered ions then pass through a 127° cylindrical electrostatic energy analyzer followed by a quadrupole radio-frequency mass spectrometer and are detected by a particle multiplier (Bendix M306). Typical angular and energy spreads for the primary ion beam are 1.5° and $0.03E_1$, respectively, where E_1 is the laboratory collision energy. Both figures represent the full widths at half-maximum.

Elastic scattering data are corrected and transformed into the center-of-mass frame of reference; the details of this procedure are discussed in Ref. 16. Care has been exercised to ensure that no stray electrons (from detachment by collisions with surfaces, etc.) are incident upon the particle multiplier. As will be pointed out later, considerable effort has been made to compare the relative elastic differential cross sections (at the same c.m. collision energy) for the two negative ions, H^- and D^-. Specifically, we have looked for slight differences in the slopes of the measured (relative) differential cross sections. For this reason long-term stability of the primary beam was essential. For all of the experiments reported here, the primary beam intensity was stable to within ±5% during the runs. The corrections applied to the laboratory data are perhaps *less certain* than 5% over the angular range utilized. However, the same systematic error (if any) would be employed when transforming laboratory intensities into c.m. cross sections for both isotopes, and hence would not appreciably alter any *difference* in the slopes of the two differential cross sections.

Some experimental effort was made to measure the kinetic-energy spectra of the detached electrons. For this purpose the radio-frequency mass spectrometer and magnetic particle multiplier were removed from the system and a Bendix Channeltron particle multiplier was inserted after the 127° electrostatic analyzer. The collision region was shielded from the magnetic fields of the primary beam electromagnet and the earth by appropriate materials. Consequently the magnetic field in the collision region was reduced to less than 0.15 G. Background electrons presumably resulting from detachment on slits were a problem and constituted an appreciable fraction of the true detached electrons when the target gas was admitted to the collision chamber. Owing to the elastic scattering of the primary beam (when the target gas was admitted), subtraction of the "background" was not thought to be particularly reliable. Consequently we are only able to report on the qualitative aspects of the detached-electron energy spectra.

IV. RESULTS: $H^-(D^-)$ + He

A. Elastic differential cross section for D^-

The relative elastic differential cross section has been measured over the energy range[17] $4.4 \leq E \leq 120$ eV, for both H^- and D^- colliding with helium. Examples of the measured relative differential cross section for D^- are shown in Figs. 3–5. The experimental measurements were performed by utilizing a variety of angular grids and under no circumstances was any fine structure observed.

The differential cross section was calculated by using Eqs. (8) and (9). The inputs necessary to calculate the differential cross section are (a) the real part of the complex potential $V_1(R)$ and (b) the imaginary portion $\Gamma(R)$. Qualitatively, the two are related in that $\Gamma(R)$ decreases to zero in the region where $V_1(R)$ crosses the relatively-well-known potential for H + He. Consequently, the first estimates for both $V_1(R)$ and $\Gamma(R)$ were guided by an assumed crossing of the two curves (denoted R_x in Fig. 1) in the vicinity of $3a_0$, as suggested by Browne and Dalgarno.[14] It was found, however, that it was not possible to fit the experimental data with such a large crossing radius; a crossing radius of $3a_0$ implies that the threshold region for detachment occurs at a rather small value of $E\theta$, less than 100 eV deg. However, in Fig. 4, it can be seen that a region of slight downward curvature in the logarithm of the differential cross section occurs for $E\theta$ in the vicinity of 200 eV deg. Interpreting this as the threshold region, we conclude that R_x must be less than $3a_0$.

In order to effect this change in R_x, a function $W(R)$ was first fitted to the calculations of Browne and Dalgarno. Subsequently a coordinate transformation was used to define $V(R)$:

$$V_1(R) = W(R+\alpha),$$

where the parameter α could be varied to adjust the crossing point R_x. Since $W(R)$ was only available for $R \geq 3a_0$, $V_1(R)$ was extended to smaller values of R by assuming a screened Coulomb form for the potential. The imaginary portion of the

complex potential was arbitrarily chosen to be a Gaussian function. By varying several of the parameters in $V_1(R)$ and $\Gamma(R)$, the calculated and observed differential cross sections could be brought into good agreement. The following functions were found to be satisfactory:

$$V_1(R)=\begin{cases}\dfrac{17.93}{R}e^{-0.564R} & R\leq 1a_0\\ \dfrac{37.26}{(R+0.3)}e^{-0.795(R+0.3)}, & 1a_0<R<3a_0\\ 33.76e^{-1.128(R+0.3)}, & R\geq 3a_0\end{cases} \tag{16}$$

$$\Gamma(R)=1.5e^{-1.61(R-1)^2}, \tag{17}$$

where the potential functions are expressed in eV and R is in bohrs. These functions along with the H+He potential are plotted in Fig. 6, where it is seen that $R_x\simeq 2.1a_0$. The functions for $V_1(R)$ in Eq. (16) as well as their first derivatives, are continuous at the two boundaries so that there are, in fact, only three independent parameters in the expression for $V_1(R)$.

The integration involed in Eq. (8) extends beyond R_x; within the framework of this model, detachment occurring in this region ($R>R_x$) can be

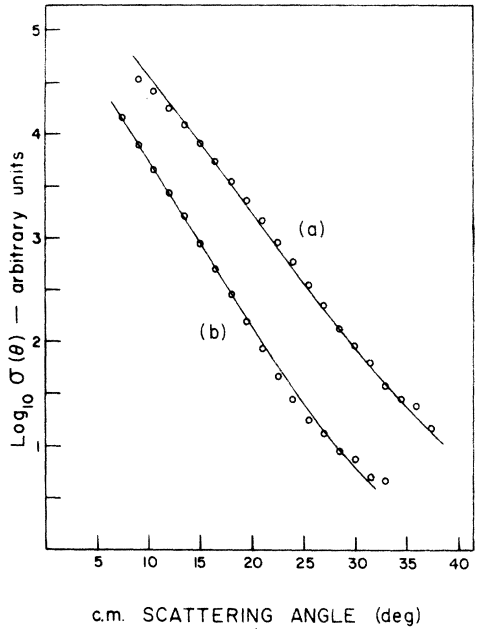

FIG. 4. Relative differential elastic scattering cross section for D^-+He. The circles are the data and the solid line is the result of a calculation which used the complex potential of Fig. 6: (a) $E_{c.m.}=16$ eV and (b) $E_{c.m.}=20$ eV.

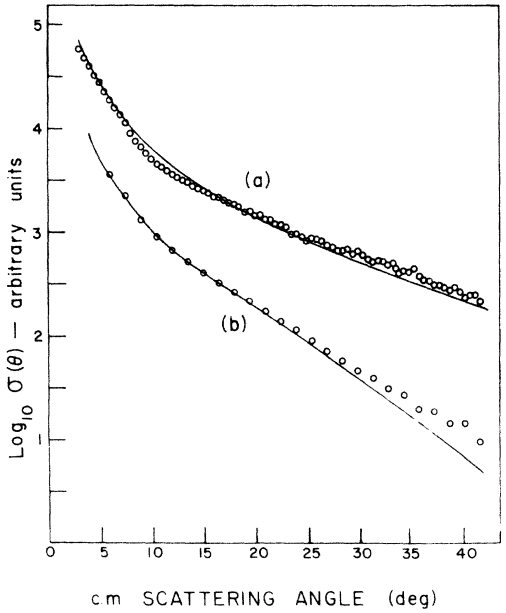

FIG. 3. Relative differential elastic scattering cross section for D^-+He. The circles are the data and the solid line is the result of a calculation which used the complex potential of Fig. 6: (a) $E_{c.m.}=4.4$ eV and (b) $E_{c.m.}=8$ eV.

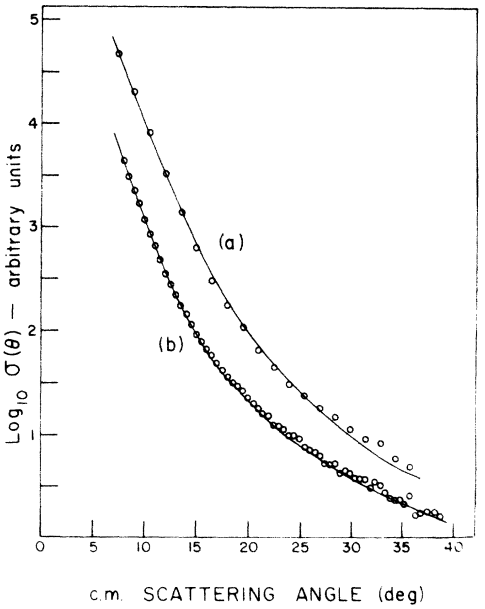

FIG. 5. Relative differential elastic scattering cross section for D^-+He. The circles are the data and the solid line is the result of a calculation which used the complex potential of Fig. 6: (a) $E_{c.m.}=34$ eV and (b) $E_{c.m.}=53$ eV.

thought of as a tunneling process. The results of calculations which use the above functions are seen along with the relevant data in Figs. 3–5. The agreement is good, and experiments with the lighter isotope also give good agreement.

The question arises as to the uniqueness of $V_1(R)$ and $\Gamma(R)$ when they are determined by this method. It is certainly possible to make small changes in the parameters of $V_1(R)$ and $\Gamma(R)$ and calculate a differential cross section which is still in good (perhaps better) agreement with the experimental results. However, both $V_1(R)$ and $\Gamma(R)$ must be physically reasonable and this places rather severe limitations on their range. $\Gamma(R)$ must go essentially to zero at R_x and it should not have a maximum of more than a few eV. $V_1(R)$ cannot be much softer or it will not cross the continuum at all. The threshold region is rather sensitive to the crossing point R_x so it cannot be appreciably altered. However, the experiments do not show whether it is better to let $\Gamma(R)$ go to zero at the crossing point or to let it extend somewhat beyond R_x. In addition, the calculated cross section is very insensitive to changes in $\Gamma(R)$ for $R \leq 1$, because there is little penetration into this region. This leads to considerable ambiguity concerning $\Gamma(R)$ in this region; we cannot tell whether Γ actually has a maximum or if it is monotonic.

Nevertheless, within the crossing formulation that has been utilized, it is felt that any potentials which reproduce the data cannot be markedly different [except for $\Gamma(R)$, $R \leq 1$] from those shown in Fig. 6.

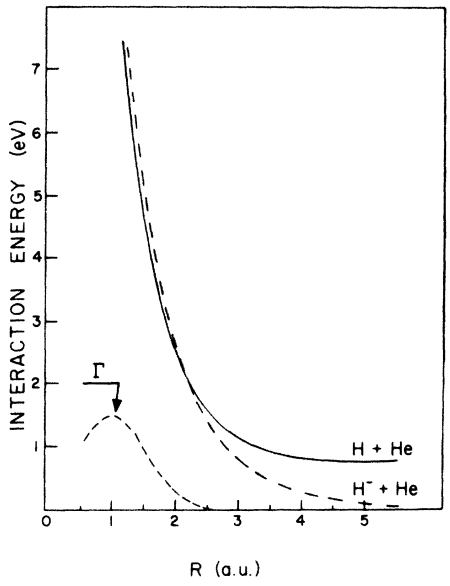

FIG. 6. Complex potential obtained from fitting data to model. The H+He interaction is obtained from Ref. 13. The analytic forms for the curves are given in the text.

B. Isotope effect

As discussed in Sec. II, the complex-potential theory predicts the isotope effect given by Eq. (11). At the same c.m. energy the differential cross section for the elastic scattering of D^- by helium should be slightly less than that for H^- by the amount:

$$\log_{10}\sigma_H(\theta) - \log_{10}\sigma_D(\theta) = \frac{(\sqrt{\mu_D} - \sqrt{\mu_H})I(\theta)}{\ln 10} .$$

In the present experiment, only the relative differential cross sections are measured, but since $I(\theta)$ increases as θ increases, the experimental results can be examined for the predicted isotope effect. Since $I(\theta)$ is slowly varying over the angular range experimentally accessible, and since we measure only relative cross sections, the isotope effect is difficult to observe. We have performed a careful series of experiments for both isotopes for a c.m. collision energy of 20 eV.

In order to display the iosotpe effect the following procedure was adopted. The results of four experiments on each isotope were averaged and the relative cross sections $A\,\sigma_H(\theta)$ and $B\,\sigma_D(\theta)$ were determined. The difference $y(\theta)$, where

$$y(\theta) = \log_{10}\sigma_H(\theta) - \log_{10}\sigma_D(\theta) + C ,$$

and C is an unknown (positive or negative) constant, was then computed in the angular range of the experiment. In order to eliminate the effect of the constant C, the deviation $Y(\theta) = y(\theta) - \bar{y}(\theta)$ is compared to a similar quantity computed by means of the complex-potential formalism. The results can be seen in Fig. 7, where both $Y_{expt}(\theta)$ and $Y_{calc}(\theta)$ are plotted as a function of θ. The magnitude of the observed isotope effect (as measured in this manner) is seen to be quite small; note that the ordinate scale for Fig. 7 is only one-tenth of those for Figs. 3–5. The error bars indicated in $Y_{expt}(\theta)$ represent the range of values obtained by comparing individual pairs of experiments. In spite of the rather large uncertainties involved, the agreement between the experiment and theory is reasonable.

C. Preliminary measurement of the detached-electron current

An attempt was made to measure the energy spectrum and the angular distribution of the detached electrons. However, as we have already mentioned, the apparatus is not especially suitable for this type of measurement; the resolution is not satisfactory, and a significant fraction of the electron current results from the collisions of

the ions with surfaces of slits. Therefore, the results have only qualitative significance.

The theoretical result for $E = 15$ eV was calculated from Eq. (14) using the known HeH potential and V_1 and Γ as determined from our elastic scattering experiments (Fig. 8). Because Γ is large, the electron energy distribution is narrow; the most probable electron energy is about 0.04 eV, and very few electrons have more than 0.5 eV. Since Γ is finite at R_x, the theoretical cross section is finite at $\epsilon = 0$. Obviously the theory is not reliable on this point; the semiclassical framework used in the derivation of Eq. (14) cannot rigorously account for classically forbidden detachment occurring at $R > R_x$.

The preliminary experimental result at a collision energy of 15 eV and a laboratory scattering angle of 11° is also shown in Fig. 8. It also shows a narrow distribution. This electron energy spectrum was obtained by setting the energy analyzer bandpass at 7.2 eV and accelerating the slow electrons to this energy. Similar measurements made with higher bandpass settings have established that the width of the measured spectrum is determined by the energy resolution of the analyzer. Therefore, the true width is less than that indicated by the data.

The measured spectrum has a maximum in the vicinity of 0.5 eV, compared to the calculated value of 0.04 eV. In these preliminary studies the residual magnetic field in the collision region of the apparatus was approximately 0.15 G, and the detached electrons drift on the order of 4 cm before being accelerated. Therefore, those electrons with energies less than 0.3 eV are defocused and their transmission through the analyzer is totally uncertain. It is likely, therefore, that the present experimental arrangement fails to detect very low-energy electrons. It should also be noted that if Γ were to go to zero linearly at R_x, then $\sigma_d(\epsilon \to 0)$ would go to zero, and the peak in the electron energy spectrum would shift to larger ϵ, giving better agreement with the experiment.

Measurements of the electron energy spectrum were made at various scattering angles. The data show large peaks at small laboratory scattering angles ($\theta < 6°$), which we attribute to apparatus effects; otherwise, the distribution seems to be essentially isotropic.

No definitive conclusions can be drawn from these results except that the electron energy and angular distributions are not incompatible with the complex-potential theory. We hope to have a much improved set of measurements in the not too distant future.

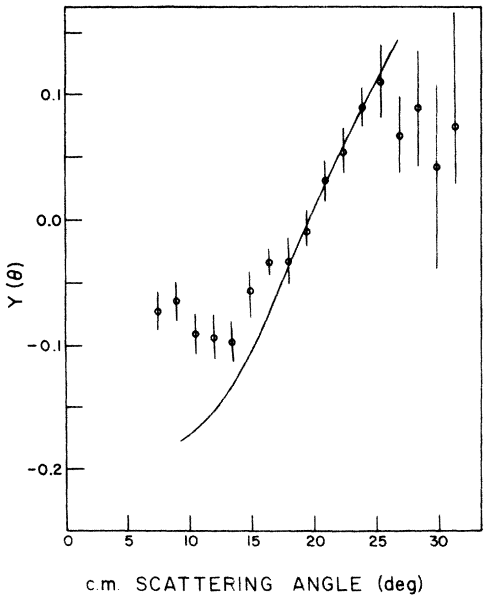

FIG. 7. Isotope effect illustrated for D^- and H^- elastic scattering for $E = 20$ eV. The quantity $Y(\theta)$ is defined in the text. The open circles are the experimental results and the solid curve is the prediction of the complex-potential model. The large uncertainties for large scattering angles are due to taking differences of very small signals.

D. Total electron-detachment cross section

In the semiclassical framework, the total cross section for electron detachment is given by

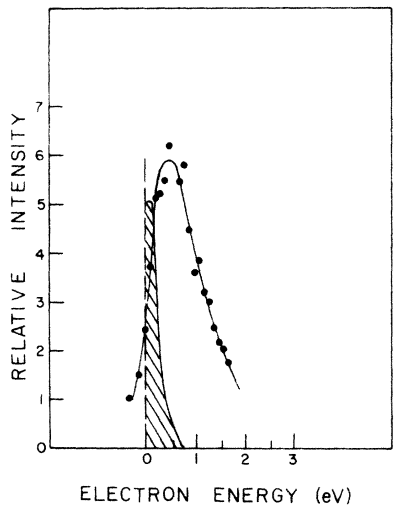

FIG. 8. Detached-electron energy spectrum for a collision energy of 15 eV (D^- + He). The shaded area is the prediction of Eq. (12) and the circles are the experimental results.

$$\sigma_{\text{tot}} = 2\pi \int_0^{\pi} [1 - P_s(\theta)]\sigma_0(\theta) \sin\theta \, d\theta$$

$$= 2\pi \int_0^{\infty} [1 - P_s(b)] b \, db \, .$$

If $\Gamma(R)$ were to go linearly to zero at R_x, the integral would vanish beyond the corresponding value of impact parameter b_x. In the present case, however, Γ allows some "classically forbidden" detachment to take place so the b integration must extend slightly beyond b_x.

The calculated result is compared with the experimental data of Bailey, May, and Muschlitz[18] in Fig. 9. The immediately obvious conclusion is that the calculated curve does not account for the large observed detachment cross section for energies above 100 eV. In this range, the calculated curve is decreasing approximately as $E^{-1/2}$, while the experimental curve gradually rises. Part of the discrepancy results from the production of protons by detachment of both electrons from H^-; this is not considered in our calculation. In addition, there is a small contribution to the experimental result from autoionizing states. If these were taken into account in the complex-potential framework, it is not clear whether the theory would account for the observations.

On the other hand, when the results are compared at low energies, they do not appear to be incompatible. In Fig. 10, the same results are shown in the low-energy region ($E < 80$ eV). Although the two results are not identical, the discrepancies are not too great, and the calculated curve with its attendant uncertainties may lie within the range of experimental uncertainties.

It should be pointed out that if R_x were as large as $3a_0$, the resulting total detachment cross section would be considerably larger than that measured by Bailey *et al.*

V. DISCUSSION

There are a number of questions concerning the complex-potential theory, not all of which have been answered by the present study. First, it is not obvious that the He-H^- curve necessarily must cross the continuum, though the calculations of Browne and Dalgarno[14] and preliminary results of Junker[5] indicate a crossing at about $3a_0$. There is no theory yet available to describe the situation if the curves do not cross.

Even if the curves do cross, there remain many questions about the applicability of the complex-potential theory. For the He-H^- system, we have no reason to expect a long-lived state, since there is no obvious potential barrier preventing electrons from escaping and there is no excited state of HeH nearby that would give rise to a Feshbach resonance. Furthermore, if the width of the resonance is comparable to the energy separation between neutral- and negative-ion curves, the complex-potential theory may be meaningless.

It should be noted that the complex-potential theory has never been derived from first principles in a completely satisfying way. One approach has been developed by Bardsley, Herzenberg, and Mandl,[1] but it is believed to apply only if the resonance is not too broad.[19] A more complicated approach, developed by Chen and co-workers,[3,4] leads to a complex potential that is not only energy dependent, but nonlocal. A totally different

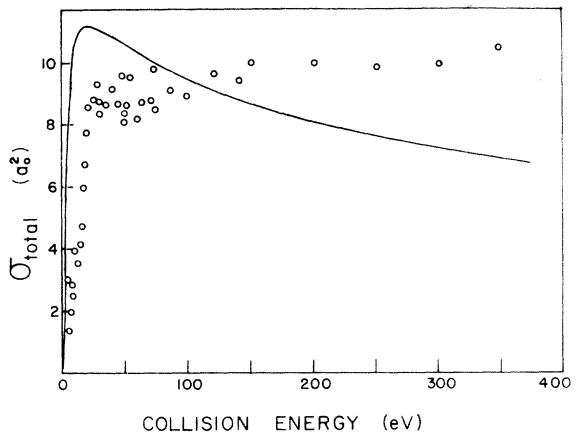

FIG. 9. Total cross section for electron detachment for H^-+He. The circles are the data of Ref. 18 and the solid line is the calculated cross section. The abscissa is the laboratory collision energy.

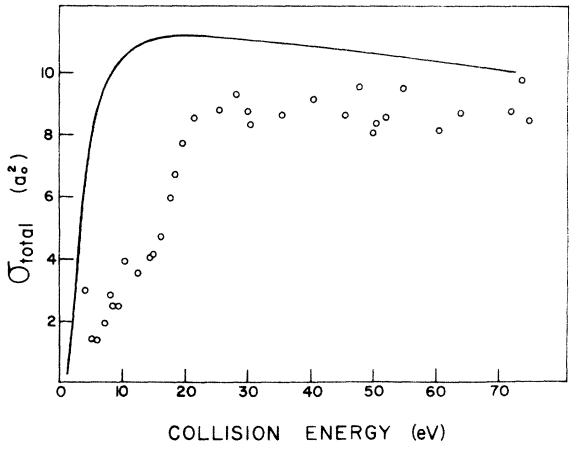

FIG. 10. Total cross section for electron detachment for H^-+He. The circles are the data of Ref. 18 and the solid line is the calculated cross section. The abscissa is the laboratory collision energy.

and much more heuristic approach has been taken by Demkov[15]; it leads to formulas quite different from Eqs. (11) through (15). The detachment problem could also be described in the more conventional framework of nonadiabatic effects, analogous to the description of two-discrete-state curve crossings. However, this approach has not yet been developed. Our point is not that the theory is invalid or inapplicable, but only that the limits of its validity and applicability are not yet known.

The present experiments and calculations lead to two conclusions. First, for the H^--He and D^--He systems, the calculations fail to describe electron-detachment processes if the incident ion energy is above 100 eV. This fact is manifested most clearly in the behavior of the total detachment cross section; the theoretical curve falls off approximately as $E^{-1/2}$, while the experimental curve is gradually rising.[6,18] Furthermore, the complex potential obtained from fitting our low-energy elastic differential scattering data does not satisfactorily predict the differential scattering data for collision energies above approximately 80 eV. Specifically, it is observed that a larger Γ is necessary to fit the high energies. These high-energy discrepancies are not surprising; the complex-potential theory would be expected to apply only to nearly adiabatic collisions. A fast collision involving a negative ion having a loosely bound electron would have to be described by some sort of direct-impact theory, or binary-encounter approximation. Also, the calculations have neglected the effects of discrete autoionizing states, and the possibility of proton production through detachment of both of the H^- electrons. These processes become significant at high energies, but their contribution at 100 eV is not known.

Second, for these systems, for energies less than 80 eV, the experimental results are generally compatible (or at least not incompatible) with the complex-potential theory. The elastic scattering differential cross sections are in good agreement with the calculations. [Of course, this by itself is not conclusive, since those experiments were used to determine $V_1(R)$ and $\Gamma(R)$.] The preliminary measurement of the electron energy and angular distribution gives results that are not incompatible with the theory. Perhaps the weakest link in the chain is the comparison of the experimental total detachment cross section with that calculated from $V_1(R)$ and $\Gamma(R)$ as determined above. Here there is some discrepancy at low energies, but not enough to refute the theory. The strongest argument in favor of the complex-potential theory is the experimental observation of the theoretically predicted isotope effect: any alternative theory of electron detachment that might be proposed would probably give a different velocity dependence to the detachment probability, and hence a different isotope effect.

Two steps can be taken to lead to a more definitive test of the theory. First, the He-H^- potential and $\Gamma(R)$ can be calculated *ab initio*. An accurate calculation can unequivocally locate a crossing point, if one exists, and remove all uncertainties in the shape of the curves. Second, we hope to have an improved measurement of the electron energy- and angular-distribution in the near future. In addition to testing the complex-potential theory, this could provide additional information on the precise behavior of Γ near R_x

APPENDIX: A SIMPLE APPROXIMATION TO THE ELECTRON-DETACHMENT CROSS SECTION

In this Appendix, we make some approximations that allow $\sigma_d(\epsilon)$ to be expressed in closed form. Although Eq. (15) permits calculation by computer, the forms presented below allow quick first-order estimates to be made of $\sigma_d(\epsilon)$. In addition, they provide a simple parametrization that may be useful in interpreting experimental data. But most important, the approximate forms make much clearer the nature and limitations of the classical theory.

In the calculation of the electron energy spectrum, it is essential to take $\Gamma(R)=0$ for $R \geq R_x$; otherwise the classical calculation would predict a finite current of electrons having negative kinetic energy ϵ. For $R<R_x$ we may take a linear approximation to Γ:

$$\Gamma(R) = \beta + \gamma(R_x - R) . \tag{A1}$$

It is not known at present whether it is better to take β to be zero or some small positive constant. We shall show the consequences of both assumptions.

Likewise, we may assume $\epsilon(R)$ is linear

$$\epsilon(R) = \delta(R_x - R) , \qquad \delta \equiv \Delta F = -\frac{d}{dR}(V_1 - V_2)\big|_{R=R_x} . \tag{A2}$$

Finally, we assume that the radial velocity is constant outside the turning point, which we take to be equal to the impact parameter,

$$v(R) = v_\infty , \quad R > R_0$$

and (A3)

$$R_0 = b .$$

The constant radial velocity approximation is rather severe, but it is commonly used in studying discrete excitations inasmuch as it is implicitly

assumed in the Landau-Zener formula.

Using these approximations in Eq. (14), we immediately obtain for the probability of detachment of an electron of energy ϵ on the incoming or outgoing part of the trajectory with impact parameter b,

$$P^{\text{in}}(\epsilon, b) = \left(\frac{\beta+\gamma\epsilon/\delta}{\delta v_\infty}\right) \exp\left[\frac{-1}{v_\infty}\left(\frac{\gamma\epsilon^2}{2\delta^2}+\frac{\beta\epsilon}{\delta}\right)\right],$$

$$P^{\text{out}}(\epsilon, b) = \left(\frac{\beta+\gamma\epsilon/\delta}{\delta v_\infty}\right) \exp\left\{\frac{1}{v_\infty}\left[\left(\frac{\gamma\epsilon^2}{2\delta^2}+\frac{\beta\epsilon}{\delta}\right) - 2\left(\frac{\gamma\epsilon_0^2}{2\delta^2}+\frac{\beta\epsilon_0}{\delta}\right)\right]\right\}, \tag{A4}$$

where v_∞ is taken to be positive in both cases, and $\epsilon_0 = \delta(R_x - b)$ represents the maximum energy the electron could achieve for a given nuclear trajectory.

The cross sections are obtained by integrating over impact parameters up to the maximum value of b that can lead to production of electrons of energy ϵ:

$$b_{\max}(\epsilon) = R_x - \epsilon/\delta. \tag{A5}$$

Thus

$$\sigma^{\text{in, out}}(\epsilon) = 2\pi \int_0^{b_{\max}(\epsilon)} P^{\text{in, out}}(\epsilon, b) b\, db \tag{A6}$$

and

$$\sigma_d(\epsilon) = \sigma^{\text{in}}(\epsilon) + \sigma^{\text{out}}(\epsilon). \tag{A7}$$

The result is, for $\epsilon \leq \delta R_x$,

$$\sigma^{\text{in}}(\epsilon) = \pi\left(R_x - \frac{\epsilon}{\delta}\right)^2 \left(\frac{\beta+\gamma\epsilon/\delta}{\delta v_\infty}\right) \exp\left[\frac{-1}{v_\infty}\left(\frac{\gamma\epsilon^2}{2\delta^2}+\frac{\beta\epsilon}{\delta}\right)\right],$$

$$\sigma^{\text{out}}(\epsilon) = \pi\left(\frac{\beta+\gamma\epsilon/\delta}{\delta v_\infty}\right) \exp\left[\frac{1}{v_\infty}\left(\frac{\gamma\epsilon^2}{2\delta^2}+\frac{\beta\epsilon}{\delta}\right)\right] \exp\left(\frac{\beta^2}{\gamma v_\infty}\right)\left\{\left(\frac{\pi v_\infty}{\gamma}\right)^{1/2}\left(R_x+\frac{\beta}{\gamma}\right) \times[\text{erf}(\eta_1) - \text{erf}(\eta_2)] + \left(\frac{v_\infty}{\gamma}\right)[\exp(-\eta_1^2) - \exp(-\eta_2^2)]\right\}, \tag{A8}$$

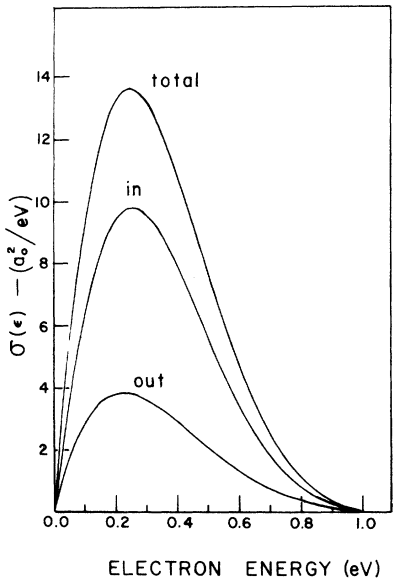

FIG. 11. Electron energy spectrum from Eq. (A8). Cross section for detachment occurring on the incoming and outgoing part of the trajectory and the total detachment for given electron energy. The collision energy is 20 eV.

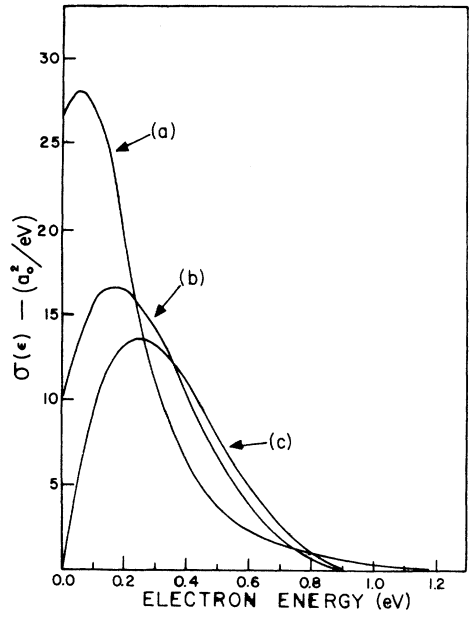

FIG. 12. Electron energy spectrum: (a) Exact result of Eq. (15); (b) Linear potentials and constant velocity approximation, from Eq. (A8), with $\beta \neq 0$; (c) Linear potentials and constant velocity, with $\beta = 0$. The approximations are generally within a factor of two of the exact result. If $\beta = 0$, $\sigma(\epsilon \to 0) = 0$.

where

$$\eta_1 = \frac{\beta + \gamma R_x}{(v_\infty \gamma)^{1/2}},$$

$$\eta_2 = \frac{\beta + \gamma \epsilon/\delta}{(v_\infty \gamma)^{1/2}}.$$

The error function is that defined in Abramowitz and Stegun. For $\epsilon > \delta R_x$, $\sigma^{in} = \sigma^{out} = 0$.

With the above expression, σ^{out} can be easily evaluated provided one has a table of the error function. The expression for σ^{in} is quite simple. The first two factors represent the geometrical cross section, πb_{max}^2, the third factor is the value of Γ, representing the rate of detachment at that point, and the exponential represents the probability that detachment has not already occurred.

Several things are immediately evident from the form of σ^{in}. First, for large Γ, i.e., large β or γ, the electron energy distribution is narrow, while for small Γ it is wide. The width increases with increasing ion velocity, and it can be shown that the maximum of $\sigma^{in}(\epsilon)$ occurs at

$$\epsilon = \text{const} \times E_{ion}^{1/4}.$$

If $\beta = 0$, then $\sigma_d\ (\epsilon = 0) = 0$, while if β is not zero, $\sigma_d(\epsilon = 0)$ is finite. Finally, $\sigma_d(\epsilon)$ goes to zero quadratically as ϵ goes to $\epsilon_{max} = \delta R_x$. These results are shown in Figs. 11 and 12.

Two questions will be of special interest in future experimental studies. First, what is the behavior of $\sigma_d(\epsilon)$ as $\epsilon \to 0$? Although the complex-potential theory cannot completely rigorously describe classically forbidden detachment occurring outside the crossing point, it might lead to reasonable results in many cases. Second, what is the behavior of $\sigma_d(\epsilon)$ as ϵ goes to ϵ_{max}? The present approximations lead to a quadratic behavior. However, if the linear approximation to $\epsilon(R)$ is removed, $\sigma_d(\epsilon)$ acquires a long tail, except at very low incident ion energies. But if a more realistic turning point is assumed, $\sigma_d(\epsilon)$ goes linearly to zero at ϵ_{max}. On the other hand, a quantum solution must lead to an exponential tail. Experiments and a quantum description of these processes will be especially interesting.

---

†Work supported in part by the National Science Foundation and NASA Grant No. NASA-NGL-47-006-058.

[1]J. N. Bardsley, A. Herzenberg, and F. Mandl, Proc. Phys. Soc. Lond. 89, 305 (1966); 89, 321 (1966).

[2]J. N. Bardsley, Proc. Phys. Soc. Lond. 91, 300 (1967); A. Herzenberg, Phys. Rev. 160, 80 (1967).

[3]J. Mizuno and J. C. Y. Chen, Phys. Rev. 187, 167 (1969); Phys. Rev. A 4, 1500 (1971); J. C. Y. Chen, *Advances in Radiation Chemistry*, edited by M. Curton and J. L. Magee (Wiley-Interscience, New York, 1968), Vol. 1, pp. 245ff.

[4]J. C. Y. Chen, Phys. Rev. 156, 12 (1967); J. C. Y. Chen and J. L. Peacher, Phys. Rev. 163, 103 (1967); 167, 30 (1968).

[5]B. Junker (private communication).

[6]J. S. Risley, Ph. D. thesis (University of Washington, 1973) (unpublished); J. S. Risley and R. Geballe, Phys. Rev. Lett. 29, 904 (1972).

[7]D. R. Bates, Phys. Rev. 78, 492 (1950); E. Bauer and T. Y. Wu, Can. J. Phys. 34, 1436 (1956).

[8]A. D. Danilov, *Chemistry of the Ionosphere* (Plenum, New York, 1970); F. C. Fehsenfeld *et al.*, J. Chem. Phys. 45, 1844 (1966); A. L. Schmeltekopf *et al.*, Astrophys. J. 148, L155 (1967); F. C. Fehsenfeld *et al.*, Planet. Space Sci. 15, 373 (1967); E. E. Ferguson *et al.*, Space Res. 7, 135 (1967).

[9]W. J. Miller, technical report No. TP-278, Aero-Chem Research Laboratories, Princeton, N. J.; D. E. Jensen, Trans. Faraday Soc. 65, 2123 (1969); J. Chem. Phys. 52, 3305 (1970); D. E. Jensen and W. J. Miller, J. Chem. Phys. 53, 3287 (1970); W. J. Miller, J. Chem. Phys. 57, 2354 (1972).

[10]D. L. Morgan and V. W. Hughes, Phys. Rev. D 2, 1389 (1970); J. N. Bardsley (to be published).

[11]A. Dalgarno and R. A. McCray, Astrophys. J. 180, 473 (1973).

[12]W. Pieper and W. Greiner, Z. Phys. 218, 327 (1969); B. Müller, H. Peitz, J. Rafelshi, and W. Greiner, Phys. Rev. Lett. 28, 1235 (1972); B. Müller, J. Rafelshi and W. Greiner, Z. Phys. 257, 62 (1967); also see recent reports of work prior to publication.

[13]See Christian Hahn, Ph. D. thesis (Max-Plank-Institute für Strömungsforschung, Berlin, 1972) for an excellent summary.

[14]J. C. Browne and A. Dalgarno, technical report No. GCA-TR-68-16-G or DASA-2148 (unpublished).

[15a]Much of this semiclassical theory was developed by W. H. Miller, J. Chem. Phys. 32, 3563 (1970).

[15b]Yu. N. Demkov, Zh. Eksp. Teor. Fiz. 46, 1126 (1964) [Sov. Phys.—JETP 19, 762 (1964); Zh. Eksp. Teor. Fiz. 49, 885 (1965) [Sov. Phys.—JETP 22, 615 (1966)]. Also see Yu. N. Demkov, G. F. Drukarev, and V. V. Kuchinskii, Zh. Eksp. Teor. Fiz. 58, 944 (1970) [Sov. Phys.—JETP 31, 509 (1970)]; J. C. Browne and A. Dalgarno, J. Phys. B 2, 885 (1969).

[16]R. L. Champion, L. D. Doverspike, W. G. Rich, S. M. Bobbio, Phys. Rev. A 2, 2327 (1970).

[17]All energies and angles refer to the center-of-mass reference frame unless stated otherwise.

[18]T. L. Bailey, C. J. May, and E. G. Muschlitz, J. Chem. Phys. 26, 1146 (1957).

[19]J. N. Bardsley (private communication).